J Periodontal Implant Sci. 2017 Dec;47(6):388-401
https://doi.org/10.5051/jpis.2017.47.6.388
pISSN 2093-2278·eISSN 2093-2286

JPIS
Journal of Periodontal & Implant Science

Research Article

Check for updates

Physicochemical characterization of porcine bone-derived grafting material and comparison with bovine xenografts for dental applications

Jung Heon Lee [1,2,*], **Gyu Sung Yi** [1], **Jin Woong Lee** [1], **Deug Joong Kim** [1,*]

[1]School of Advanced Materials Science and Engineering, Sungkyunkwan University, Suwon, Korea
[2]SKKU Advanced Institute of Nanotechnology, Sungkyunkwan University, Suwon, Korea

OPEN ACCESS

Received: Nov 1, 2017
Accepted: Dec 22, 2017

***Correspondence:**
Jung Heon Lee
School of Advanced Materials Science and Engineering, Sungkyunkwan University, 2066 Seobu-ro, Jangan-gu, Suwon 16419, Korea.
E-mail: jhlee7@skku.edu
Tel: +82-31-290-7404
Fax: +82-502-302-1918

Deug Joong Kim
School of Advanced Materials Science and Engineering, Sungkyunkwan University, 2066 Seobu-ro, Jangan-gu, Suwon 16419, Korea.
E-mail: kimdj@skku.edu
Tel: +82-31-290-7394
Fax: +82-31-290-7410

ORCID iDs
Jung Heon Lee
https://orcid.org/0000-0003-4790-3525
Gyu Sung Yi
https://orcid.org/0000-0001-6367-7295
Jin Woong Lee
https://orcid.org/0000-0002-8253-8677
Deug Joong Kim
https://orcid.org/0000-0003-2449-3893

ABSTRACT

Purpose: The physicochemical properties of a xenograft are very important because they strongly influence the bone regeneration capabilities of the graft material. Even though porcine xenografts have many advantages, only a few porcine xenografts are commercially available, and most of their physicochemical characteristics have yet to be reported. Thus, in this work we aimed to investigate the physicochemical characteristics of a porcine bone grafting material and compare them with those of 2 commercially available bovine xenografts to assess the potential of xenogenic porcine bone graft materials for dental applications.
Methods: We used various characterization techniques, such as scanning electron microscopy, the Brunauer-Emmett-Teller adsorption method, atomic force microscopy, Fourier-transform infrared spectroscopy, X-ray diffraction, and others, to compare the physicochemical properties of xenografts of different origins.
Results: The porcine bone grafting material had relatively high porosity (78.4%) and a large average specific surface area (SSA; 69.9 m^2/g), with high surface roughness (10-point average roughness, 4.47 μm) and sub-100-nm hydroxyapatite crystals on the surface. Moreover, this material presented a significant fraction of sub-100-nm pores, with negligible amounts of residual organic substances. Apart from some minor differences, the overall characteristics of the porcine bone grafting material were very similar to those of one of the bovine bone grafting material. However, many of these morphostructural properties were significantly different from the other bovine bone grafting material, which exhibited relatively smooth surface morphology with a porosity of 62.0% and an average SSA of 0.5 m^2/g.
Conclusions: Considering that both bovine bone grafting materials have been successfully used in oral surgery applications in the last few decades, this work shows that the porcine-derived grafting material possesses most of the key physiochemical characteristics required for its application as a highly efficient xenograft material for bone replacement.

Keywords: Bioprosthesis; Chemical phenomena; Dental materials; Durapatite; Heterografts

Funding

This work was supported by the National Research Foundation of Korea (NRF) funded by the Ministry of Science, ICT & Future Planning, Korea (Grant number: 2017M3C1B7014335).

Author Contributions

Conceptualization: Jung Heon Lee, Deug Joong Kim; Formal analysis: Jung Heon Lee, Gyu Sung Yi, Jin Woong Lee; Investigation: Jung Heon Lee, Gyu Sung Yi, Jin Woong Lee; Methodology: Jung Heon Lee, Gyu Sung Yi, Jin Woong Lee, Deug Joong Kim; Writing - original draft: Jung Heon Lee; Writing - review & editing: Jung Heon Lee, Gyu Sung Yi, Deug Joong Kim.

Conflict of Interest

No potential conflict of interest relevant to this article was reported.

INTRODUCTION

Bone grafting is a surgical procedure frequently performed in orthopedics and periodontics to treat patients with missing or damaged bones. Bone grafting not only helps to fill the physical gaps created by the missing or damaged bone and provides structural stability, but also stimulates the growth of bone tissues. In particular, periodontal bone grafts improve clinical outcomes in oral and maxillofacial surgery.

Although graft materials prepared from natural bones of different origin are mostly composed of hydroxyapatite (HA), because of its high biocompatibility and osteoconductivity, their performance is known to be significantly affected by their physicochemical properties [1]. For example, as autologous graft materials originate from the patient's own bone and can be used with minimal treatment, they have been reported to be the most efficient and fastest-healing bone substitute materials. In contrast, allografts are known to be not as effective as autografts, because the extensive chemical treatments required to prevent potential infectivity (e.g., from human immunodeficiency virus [HIV] and hepatitis viruses) can disrupt the hierarchical structure of bone and remove a significant amount of the growth factors necessary for efficient bone regeneration.

Physicochemical properties are even more important for xenografts [2]. Xenografts have clear advantages, as they can be mass-produced in large quantities at relatively affordable processing costs. However, as they originate from bone tissues of other species, their native osteological characteristics are quite different from those of human bone tissues. In addition, the series of chemical processes or thermal treatments performed on xenografts can further affect their physical and chemical properties. Thus, the physicochemical characteristics of a xenograft can be closely related to its overall performance for bone regeneration.

Bovine bones were the first animal bones employed for the production of xenograft materials, and several bovine xenograft products currently dominate the market share of bone graft materials. For example, Bio-Oss® (Geistlich Biomaterials, Wolhusen, Switzerland) is a well-known xenograft, composed of an osseous mineral matrix obtained from spinal bone [3]. Cerabone® (Botiss Biomaterials GmbH, Zossen, Germany) is another popular bone grafting material obtained from cancellous bone of cattle femur condyles [4].

In contrast, porcine-derived bone graft materials have only recently been developed and marketed. It has been reported that porcine bone has a similar formulation and structure to human bone [5]. The lipid content (in terms of category and structure) of porcine bone is also similar to that of human bone [6]. In addition, porcine bone has a relatively low risk of zoonosis [7]. Thus, considerable efforts are being devoted to replacing bovine bone graft materials with materials obtained from porcine bone [7-9]. However, studies of the physicochemical characteristics of xenografts originating from porcine bone remain very limited.

Therefore, in this work, we carried out a detailed study on the physicochemical properties of a commercially available porcine xenograft, THE Graft, and compared them with the properties of the bovine-origin xenografts, Bio-Oss® and Cerabone®. We focused on the morphology/porosity, specific surface area (SSA), 3-dimensional (3D) tomography, chemical component analysis, organic content analysis, and wettability of these materials, as these are considered to be important characteristics of graft materials. The results of our study suggest that the graft material obtained from porcine bone is comparable to the materials prepared

https://doi.org/10.5051/jpis.2017.47.6.388

from bovine bone in many aspects; moreover, the present material satisfies most of the key requirements for its effective application as a xenograft material.

MATERIALS AND METHODS

Materials

THE Graft (Purgo Biologics, Seongnam, Korea), Bio-Oss® (Geistlich Biomaterials), and Cerabone® (Botiss Biomaterials GmbH) were purchased and used to compare the physicochemical properties of xenografts of different origins.

Physicochemical characterization

Morphological characterization/porosity

The morphological characterization of the materials was carried out by scanning electron microscopy (SEM) using a field emission-environmental scanning electron microscope (Philips XL-30 ESEM-FEG, Philips Corp., Eindhoven, Netherlands) operating at 15.2 kV. The pore size analysis was performed by mercury intrusion porosimetry (MIP) (Autopore V 9600, Micromeritics Instrument Corp., Norcross, GA, USA). The measurements were made using 255.9 mg of THE Graft, 138.9 mg of Bio-Oss®, and 181.2 mg of Cerabone®. The total porosity per unit mass was calculated from the total intrusion volume. Mercury was applied with a pressure of 0.10–60,000.00 psia for the measurements. The contact angle of the mercury was 130°.

SSA

The SSA was measured using a nitrogen gas porosimeter (ASAP 2420, Micromeritics Instrument Corp.) after degassing 1.0 g of each sample below 0.010 mmHg at 150°C for 5 hours. The SSA was expressed as square meters per gram of mineral (m^2/g).

3D tomography

The 3D tomography of graft materials was carried out by creating ultrathin (up to 10 nm) sections of frozen epoxy resin-reinforced graft samples with an ultramicrotome and stacking their corresponding 2-dimensional (2D) atomic force microscopy (AFM) images into a 3D image. The Japanese Industrial Standard for roughness (Rz_{JIS}) was measured based on the 5 highest peaks and lowest valleys over the entire sampling length. The sampling length was 50 μm [10,11].

Chemical characterizations

The crystalline phase composition of the samples was determined by X-ray diffraction (XRD) using a D8 Advance diffractometer (Bruker Optics, Billerica, MA, USA) operating at 40 kV and 40 mA, with Cu K_α radiation to probe the 2θ range of 20°–80°. The ground samples (less than 0.3 g) were packed in a holder and measured with the diffractometer at scan steps of 0.02°, with a time per step of 35.4 seconds. Fourier-transform infrared (FT-IR) spectroscopy (Tensor 27, Bruker Optics) was used for the chemical analysis of the graft materials. A small amount (less than 0.3 g) of each graft sample was mixed with potassium bromide powder to produce a sample pellet. FT-IR spectroscopy was performed in transmission mode.
For the elemental analysis of graft materials, inductively coupled plasma optical emission spectrometry (ICP-OES) (Optima 5300 DV, Perkin-Elmer, Waltham, MA, USA) was used. Each sample (0.1 g) was placed in a platinum crucible and dissolved at 200°C for 1 hour in nitric acid and deionized (DI) water before measurement. The ICP-OES measurements were performed based on ASTM F1581-08.

https://doi.org/10.5051/jpis.2017.47.6.388

Residual protein analysis

The residual protein content in the xenograft materials was determined using both nitrogen and amino acid analysis. For the nitrogen analysis, we first quantified the nitrogen content in the sample using an elemental analyzer (Flash EA 2000 series, ThermoFisher Inc., Cambridge, UK). We multiplied the nitrogen content by the protein factor of 6.25 to obtain the amount of protein in the sample based on the Kjeldahl method [12]. For the amino acid analysis, we first completely dried 1 mg of the sample, then hydrolyzed it with HCl at 110°C for 24 hours, and derivatized the hydrolyzed amino acids with phenylisothiocyanate. After complete drying, the samples were dissolved with 200 μL of 0.05 M sodium acetate trihydrate. After centrifugation, the supernatant was analyzed with high-performance liquid chromatography using a HP 1100 Series liquid chromatography system (Agilent, Santa Clara, CA, USA) (C18 4 μm [3.9×300 mm], spectrophotometer at 254 nm). Individual amino acids were calculated using the chromatogram obtained with a standard solution (Waters Co., Milford, MA, USA).

Wettability

Wetting mass measurements were carried out with a force tensiometer (Sigma 700, Biolin Scientific, Gothenburg, Sweden) using 0.75 g of each sample in DI water.

RESULTS

Morphology and porosity of the graft materials

All examined xenografts were in granulated form. The size distribution of the granules of graft materials was determined by counting the number of granules of different sizes after sorting them with commercially available sieves of different mesh sizes. The size of the granules of each sample was uniformly distributed within the 0.15–1 mm range, with maximum counts between 0.3 and 0.6 mm (Figure 1). This suggests that THE Graft, Bio-Oss®, and Cerabone® all had a similar particle size distribution.

To investigate the surface morphology of THE Graft, we obtained SEM images of its granules and compared them to the corresponding images obtained for Bio-Oss® and Cerabone®

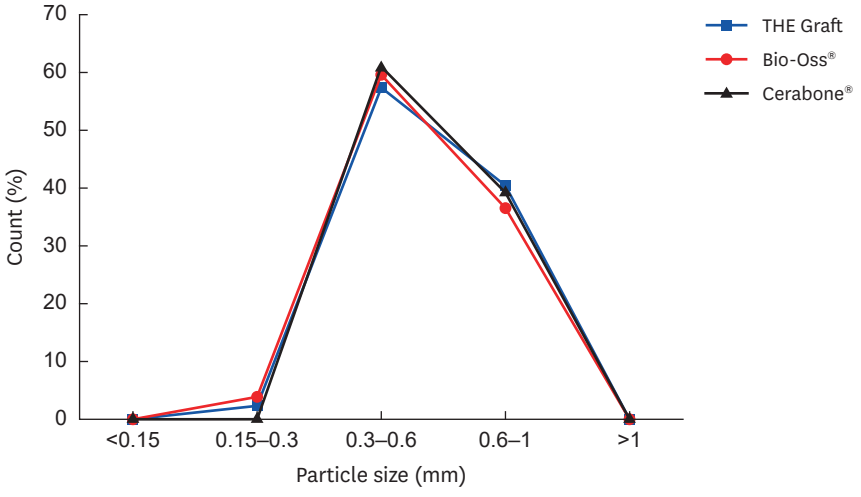

Figure 1. Size distribution of the examined xenografts.

https://doi.org/10.5051/jpis.2017.47.6.388

samples (Figure 2). As expected, the xenograft materials were predominantly found in granular form with sizes between 0.15 and 1 mm. The majority of the examined granules contained macropores (diameter >100 μm), which are necessary to form blood vessels and induce both bone growth and reorganization around the graft material. In addition, the 3 graft materials contained a large amount of micropores (diameter <10 μm), which are required for the penetration of body fluids, ion transportation, the attachment of osteoblasts, and the precipitation of newly formed HA. Further zoomed images of both THE Graft and Bio-Oss® showed that these graft materials were composed of sub-100-nm grains with a large amount of nanoscale pores present between the grains (Figure 2C and F). In contrast, sub-100-nm grains and nanoscale pores were not observed on the surface of Cerabone® (Figure 2I).

Next, we used MIP to compare the pore size distribution of the 3 xenograft materials (Figure 3). MIP is a simple and versatile technique used to measure the pore size distribution of a variety of porous materials. This technique, which is based on the capillary depression of mercury, can be used to measure a wide range of pore diameters, from 3 nm to 1,100 μm, as well as other parameters including porosity, average pore diameter, and bulk density. THE Graft had a large fraction of pore sizes in the 3–50 nm range and a non-negligible fraction

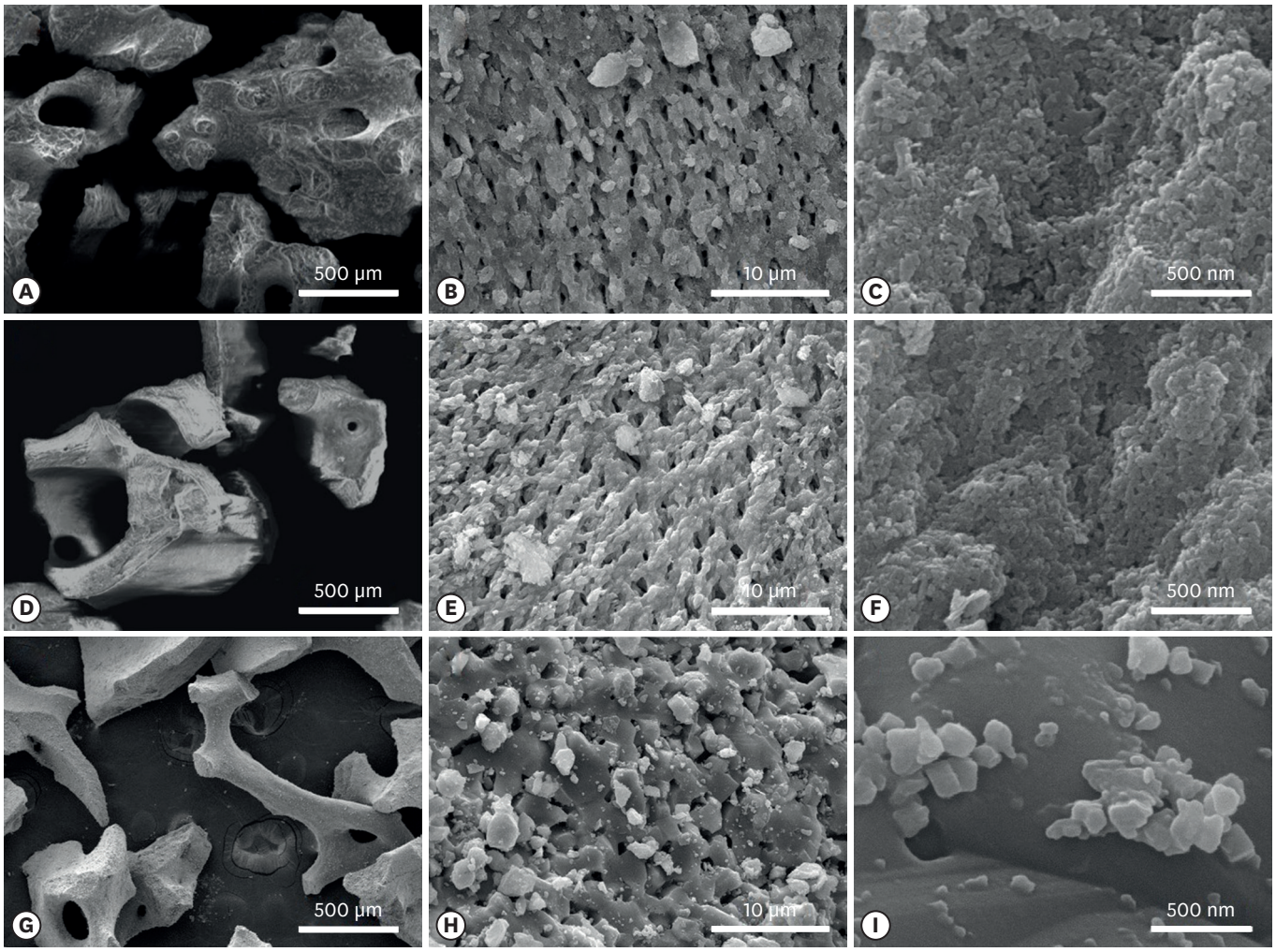

Figure 2. Surface morphologies of the xenograft materials. (A-C) THE Graft, (D-F) Bio-Oss®, and (G-I) Cerabone®.

https://doi.org/10.5051/jpis.2017.47.6.388

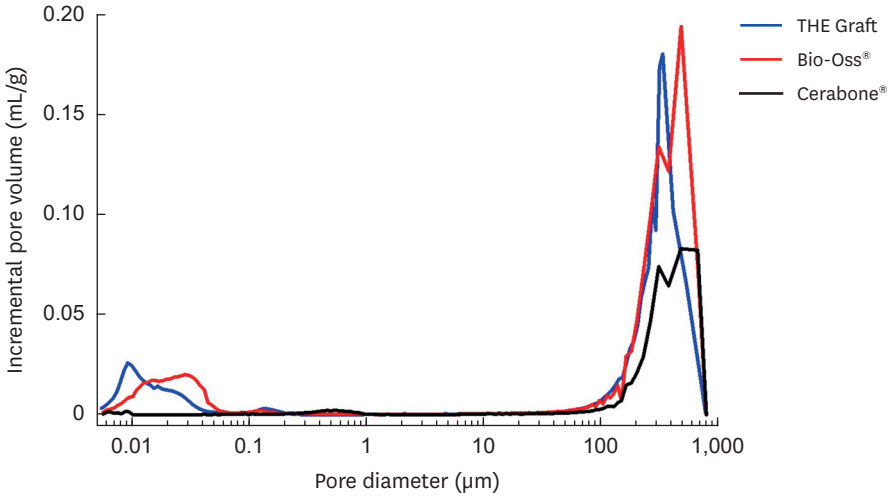

Figure 3. Pore size distribution of the graft materials.

in the 60–300 nm range. The macropores were found to be larger than 60 μm. The average pore diameter of THE Graft was 0.06 μm (Table 1). Surprisingly, Bio-Oss® showed a pore size distribution very similar to that of THE Graft, with a large fraction of pore sizes in the 3–60 nm range, some pores within the 65–280 nm range, and macropores beyond 60 μm. The average pore diameter of Bio-Oss® was also similar to that of THE Graft. In contrast, the pore size distribution of Cerabone® was significantly different from that of the other 2 materials. The Cerabone® granules had a negligible content of sub-100-nm pores: most pores were larger than 50 μm, with only a small fraction of pores between 200 nm and 1 μm. The average pore diameter of Cerabone® was 0.46 μm, which is significantly larger than that of both THE Graft and Bio-Oss®.

The porosity of THE Graft was found to be 78.4%, which is larger than that of both Bio-Oss® and Cerabone® (Table 1). Considering the comparable porosity of human trabecular bone (79.3%), this result suggests that THE Graft resembles the porous structure of human bone quite closely [13]. Since both macropores and micropores play important roles in bone formation, high porosity is crucial for the performance of graft materials [14,15]. The higher porosity of THE Graft compared with both Bio-Oss® and Cerabone® suggests that THE Graft could represent an efficient xenograft material.

SSA analysis

To measure the SSA of the present materials, we carried out a Brunauer-Emmett-Teller (BET) isotherm analysis using nitrogen gas adsorption after degassing the samples below 0.010 mmHg at 150°C for 5 hours [16,17]. The nitrogen gas adsorption technique can be used to measure many parameters related to the porosity of a sample, including pore volume, pore size distribution, and SSA.

Table 1. Porosity of the graft materials

Sample	Average pore diameter (μm)	Porosity (%)	Bulk density (g/mL)
THE Graft	0.06	78.4	0.50
Bio-Oss®	0.06	70.5	0.54
Cerabone®	0.49	62.0	1.20

https://doi.org/10.5051/jpis.2017.47.6.388

Table 2. Specific surface area

Sample	Specific surface area (m^2/g)
THE Graft	69.9±23.5
Bio-Oss®	65.4±16.7
Cerabone®	0.5±0.1

The SSA of THE Graft and Bio-Oss® were similar (Table 2). In contrast, the SSA of Cerabone® was significantly smaller than the values measured for THE Graft and Bio-Oss®. Considering that both THE Graft and Bio-Oss® had a similar surface morphology and pore size distribution with a substantial amount of nanoscale pores, whereas Cerabone® did not, we believe that this difference in the SSA was closely related to the nano/microscale structure of the bone graft materials.

3D tomography of graft materials

Roughness is an important property of graft materials, owing to its strong influence on the adhesion, growth, proliferation, and osseointegration of osteoblast cells [18]. However, measuring the roughness of a granular graft material is a very difficult task, due to its waviness, which is associated with its shape and porosity. By creating ultrathin (up to 10 nm) sections of epoxy resin-reinforced graft samples with an ultramicrotome and stacking their corresponding 2D AFM images into a 3D image, it was possible to analyze the 3D tomography of the granules of THE Graft and Bio-Oss® and to estimate their 10-point mean roughness (Rz_{JIS}) (Figure 4). We considered it especially important to characterize these 2 samples because we found that they were very similar in terms of surface morphology, total porosity, pore size distribution, and SSA.

The Rz_{JIS} of THE Graft was found to be 4.47 μm (Figure 4B). However, a parallel measurement for the Bio-Oss® sample yielded a Rz_{JIS} value of 1.37 μm, which is approximately 3 times lower than that of THE Graft. This indicates that the granules of THE Graft were rougher than those of the Bio-Oss®. Considering the significant impact of surface roughness on the performance of graft materials, this result suggests that THE Graft could represent an ideal scaffold material.

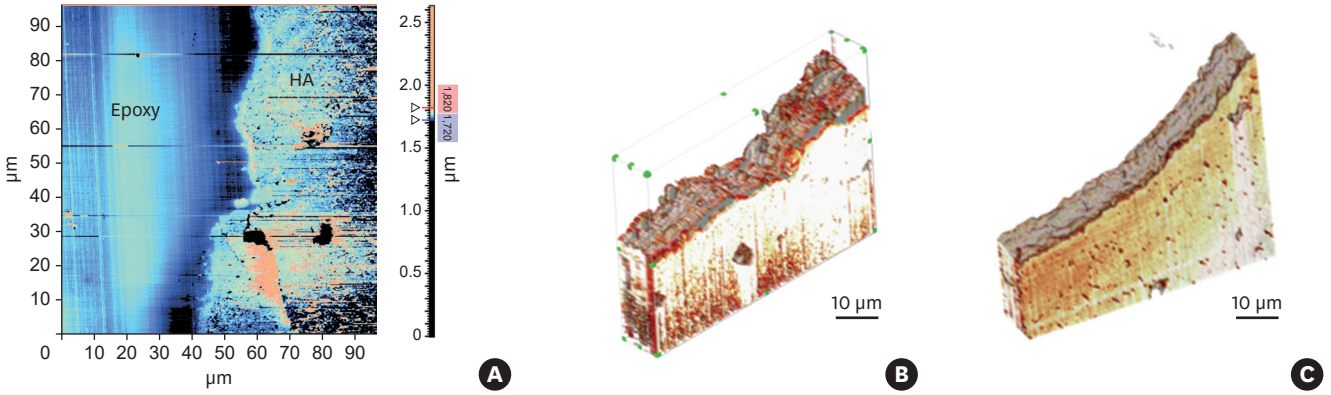

Figure 4. Measurement of the roughness of the grafting materials using 3D AFM. (A) The 2D AFM image of porcine graft section cut with an ultramicrotome. The 3D tomography of (B) THE Graft and (C) Bio-Oss® was obtained by stacking their 2D AFM images. The Rz_{JIS} roughness of the samples from THE Graft and Bio-Oss® was found to be 4.47 and 1.37 μm, respectively.
3D: 3-dimensional, 2D: 2-dimensional, AFM: atomic force microscopy, Rz_{JIS}: Japanese Industrial Standard for roughness, HA: hydroxyapatite.

https://doi.org/10.5051/jpis.2017.47.6.388

JPIS
Journal of Periodontal & Implant Science

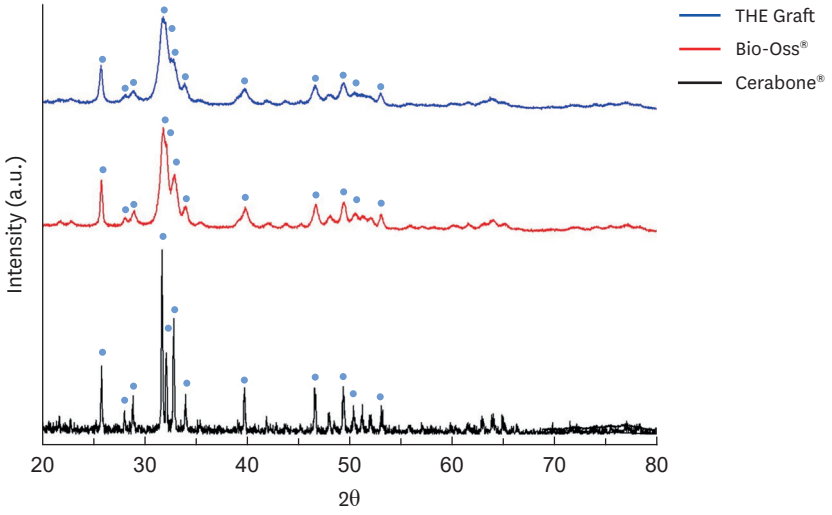

Figure 5. XRD patterns of THE Graft, Bio-Oss®, and Cerabone®. The blue dots mark the reference hydroxyapatite peaks. XRD, X-ray diffraction.

XRD analysis

XRD is frequently used to qualitatively and quantitatively characterize the chemical composition, phase identification, and crystallinity of inorganic compounds. XRD characterization has many advantages, as it can be easily carried out with a minimal sample preparation process for most powder-form samples in the air. A standard reference database is generally required to interpret data from an unknown material.

We carried out XRD analysis on THE Graft to identify its phase composition. The blue-dotted main peaks were indexed to the (002), (102), (210), (211), (112), (300), (202), (310), (222), (213), (321), and (004) planes of HA (Figure 5), respectively (JCPDS card No. 9-432), showing that THE Graft had the same crystal structure as HA ($Ca_{10}[PO_4]_6[OH]_2$) [1].

The XRD patterns of Bio-Oss® and Cerabone® showed main peaks at almost identical positions as THE Graft, suggesting that Bio-Oss® and Cerabone® were also composed of HA. Both THE Graft and Bio-Oss® had a low degree of crystallinity, whereas Cerabone® exhibited significantly stronger and narrower diffraction peaks. As HA structures with lower degree of crystallinity tend to be more degradable [19,20], this finding suggests that THE Graft and Bio-Oss® will rapidly be replaced with osteoblasts.

FT-IR analysis

The chemical composition of the graft materials and their main functional groups were investigated by FT-IR analysis (Figure 6) [21,22]. FT-IR is frequently used to study bone matrices, as their major components, such as HAs, carbonates, and collagen fibers, are known to absorb infrared radiation within the range of 500–4,000 cm^{-1}. FT-IR can therefore be used to identify the chemical composition of the inorganic component of xenograft materials and to determine whether the organic component of the natural bone is present after deproteination [23].

The FT-IR spectrum of THE Graft was very similar to that of Bio-Oss®, with PO_4^{3-} stretching bands at 415–598 and 962–1,088 cm^{-1} and the O-H stretching band centered at 3,574 cm^{-1}. We also observed H_2O absorption bands at 1,636 and 3,448 cm^{-1} and CO_3^{2-} bands at 871, 1,413,

https://doi.org/10.5051/jpis.2017.47.6.388

JPIS
Journal of Periodontal & Implant Science

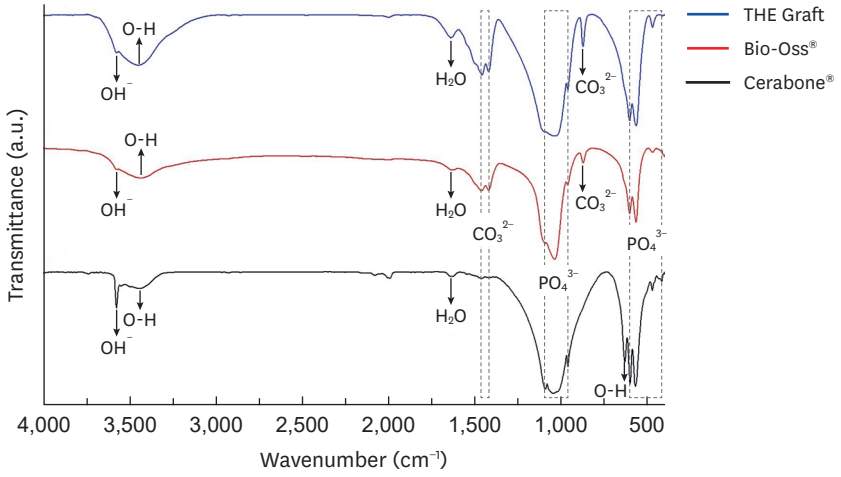

Figure 6. FT-IR spectra of (A) THE Graft, (B) Bio-Oss®, and (C) Cerabone®.
FT-IR, fourier-transform infrared.

and 1,455 cm^{-1}, which typically appear when CO_3^{2-} replaces phosphate in the apatite lattice. These results confirm the presence of HA in THE Graft and Bio-Oss®. In contrast, the FT-IR spectrum of Cerabone® was slightly different from that of the other 2 graft materials, with a significantly stronger O-H stretching band at 3,574 cm^{-1}, the O-H libration band at 632 cm^{-1}, and a much weaker CO_3^{2-} band at 871 cm^{-1}. However, insignificant organic phases, which could be identified as amide I and amide II bands at 1,634 and 1,548 cm^{-1}, respectively, were observed in the xenograft materials.

ICP-OES analysis

In order to investigate the Ca and P content of the graft materials, we carried out an elemental analysis of the graft materials using ICP-OES. We used ICP-OES because it is possible to analyze wide concentration ranges of multiple metallic or non-metallic elements existing in a variety of sample matrices with few issues with interference. Both the amounts of Ca and P were comparable between the inorganic graft materials (Table 3). An insignificant amount (<1% by weight) of Na, Mg, Zn, and Sr was detected in all 3 graft materials. The Ca/P molar ratio was similar for all 3 graft materials as well. This suggests that the Ca and P content of THE Graft was comparable to that of Bio-Oss® and Cerabone®, although they originated from bone tissues of different species.

Residual organic content analysis

The Kjeldahl method was the first technique used to determine the residual protein content in graft materials [12,24]. Although this method may not be suitable for measuring the exact protein content in a sample, it is still a standard method used to estimate the overall protein concentration in diverse types of samples. We first measured the nitrogen content present in each sample using an elemental analyzer, and then multiplied the result by the protein factor of 6.25 to estimate the protein content in the sample. No protein was detected in the samples

Table 3. Elemental analysis (ICP-OES) of the graft materials (unit: % by weight)

Element	THE Graft	Bio-Oss®	Cerabone®
Ca (%)	37.1	38.2	37.6
P (%)	19.3	19.2	19.8
Ca/P molar ratio	1.49	1.54	1.47

ICP-OES, inductively coupled plasma optical emission spectrometry.

https://doi.org/10.5051/jpis.2017.47.6.388

JPIS
Journal of Periodontal & Implant Science

Table 4. Residual organic substance analysis

Analysis	THE Graft	Bio-Oss®	Cerabone®
Kjeldahl method	Not detected	0.109%	Not detected
Amino acids	0.0158 mg/100 mg	0.0910 mg/100 mg	0.0478 mg/100 mg

of THE Graft and Cerabone® (Table 4). However, small amount of protein content could be detected in the Bio-Oss® sample. To analyze the amount of amino acid content of each xenograft sample in a more accurate manner, we used the pre-column derivatization method for amino acid analysis. This method is known to be one of most reliable ways to quantify peptides and proteins in a sample, since it has detection limit lower than picomoles and can be used to identify the amount of each common amino acid [25,26]. Bio-Oss® had the largest amount of amino acids among the 3 xenografts. This result is consistent with the results of the nitrogen analysis. Cerabone® had less amino acid content than Bio-Oss®, and THE Graft contained the lowest amino acid amount among the tested samples.

Wettability of the graft materials

Wettability is another important factor that affects the performance of a graft material. Although contact angle measurements are generally used to determine the surface energy of a flat surface, this technique is not applicable for most porous materials in granular form, such as the present graft materials. Hence, in this case we used the wicking method, based on the Washburn equation (1).

The contact angle of porous materials can be calculated by the wetting mass based on the Washburn equation (1):

$$\frac{m^2}{t} = \frac{c \cdot \rho^2 \cdot \sigma \cdot cos\theta}{2\eta} \quad (1)$$

where m is the mass increase of a test liquid with viscosity η, density ρ, and surface tension of σ as a function of the flow time t, while the capillary constant of the sample, c, is determined from the size of the granules and their packing density, to estimate the surface energies of the xenograft materials.

We plotted water mass wetting for THE Graft, Bio-Oss®, and Cerabone® as a function of time

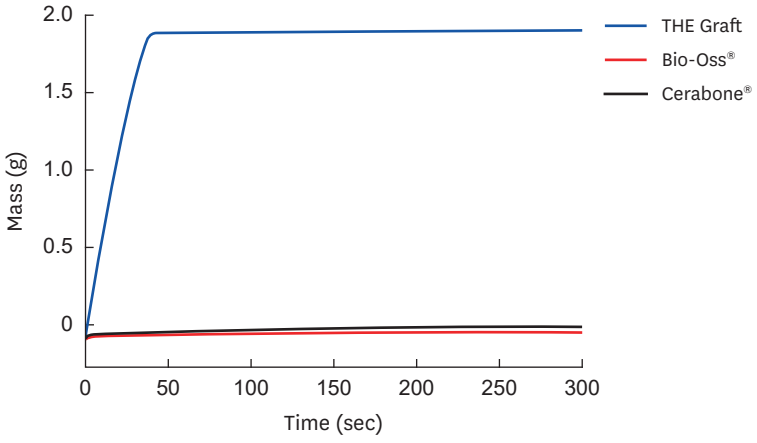

Figure 7. Wetting mass of the graft materials as a function of time.

https://doi.org/10.5051/jpis.2017.47.6.388

(Figure 7). Although Cerabone® exhibited a slightly higher wetting mass than Bio-Oss®, the wetting mass of THE Graft was considerably higher than that of the other 2 materials. Since the cosine value of the contact angle is directly related to the square of the wetting mass in equation (1), this result indicates that the wettability of THE Graft was significantly higher than that of the other 2 graft materials.

DISCUSSION

This paper summarizes comparative physicochemical characterization studies of THE Graft, Bio-Oss®, and Cerabone® that were performed to evaluate their suitability as bone void filler in dental surgery. Although both Bio-Oss® and Cerabone® originate from bovine bone, many of their properties, including the surface morphology, porosity, pore size distribution, and SSA were found to be substantially different. Bio-Oss® not only had high porosity and a large SSA, but also had nanoscale pores, which are typical characteristics of natural bone. This suggests that Bio-Oss® contains many physical characteristics of the native bovine osseous structure to a certain degree even after the deproteination process. In contrast, Cerabone® had relatively low porosity and a small SSA with negligible nanoscale pores. This indicates that a significant portion of the physical characteristics of bovine osseous structure had been altered in Cerabone®, probably due to high-temperature thermal processing procedures. Most of the physical characteristics of THE Graft, including the morphology, porosity, and SSA, were substantially equivalent to those of Bio-Oss®, despite their different origin. This suggests that THE Graft also preserves most of the physical properties of the native porcine osseous structure very well.

We believe that the different pore size distribution characterized using MIP may be closely related to the surface morphology of the graft materials composed of sub-100-nm HA grains. It is worth noting that the sub-100-nm pores observed in THE Graft and Bio-Oss® are also found in human bone, where they originate from the open gaps between HA crystals and collagen [27]. These nanoscale pores have been reported to be very important for cell adhesion, proliferation, and differentiation [19,28,29]. It should be emphasized that osteoblasts not only show better proliferation, but also synthesize alkaline phosphatase and generate calcium-containing minerals on extracellular matrix more actively, on surfaces composed of sub-100-nm HA grains [30].

The SSA, or the total surface area of a material per unit mass, is another important parameter that determines the overall behavior of a graft material. A large surface area is a key requirement for graft materials, and not only results in a larger surface region available for the attachment of osteoblast cells, but also facilitates the exchange of nutrients and waste products and allows greater amounts of blood, proteins, and growth factors to be absorbed onto the scaffold [31].

The chemical analysis using XRD, FT-IR, and ICP-OES demonstrated that THE Graft was mainly composed of HA and showed that its chemical composition, major functional groups, and Ca/P molar ratio were very similar to those of Bio-Oss® and Cerabone®. These results indicate that chemical properties of this porcine-origin xenograft are not significantly different from those of the bovine-origin graft materials. However, it is noteworthy that the degree of crystallinity of both THE Graft and Bio-Oss® was somewhat lower than that of Cerabone®, which might facilitate the efficient replacement of graft materials with bone

https://doi.org/10.5051/jpis.2017.47.6.388

tissue. The wettability of THE Graft turned out to be higher than that of both Bio-Oss® and Cerabone®, which suggests that THE Graft is relatively hydrophilic and can be easily wet by body fluids after implantation. Not only protein adsorption, but also the attachment, growth, and proliferation of various types of cells, including osteoblasts, have been reported to be significantly affected by the wettability of the material surface [32]. Thus, high-energy surfaces are generally known to be highly beneficial for dental materials [33]. This high wettability of THE Graft suggests that it may have advantages in terms of protein adsorption and the resulting cell adhesion and proliferation processes after implantation. The content of the organic component of THE Graft was somewhat lower than that of both Bio-Oss® and Cerabone®. These results show that organic substances, including collagen and other organic compounds, were successfully removed from THE Graft, which is thus not affected by issues associated with the organic content.

According to the results presented in this paper, the porcine-derived THE Graft material has most of the key physicochemical characteristics required for it to be applied as a highly efficient xenograft material for bone replacement. Both Bio-Oss® and Cerabone® have been successfully used in oral surgery in the last few decades, and have gained a substantial market share. Therefore, it is expected that THE Graft, a porcine-derived xenograft, will perform as effectively as Bio-Oss® and Cerabone® as a bone void filler in oral surgical applications.

REFERENCES

1. Park SY, Kim KI, Park SP, Lee JH, Jung HS. Aspartic acid-assisted synthesis of multifunctional strontium-substituted hydroxyapatite microspheres. Cryst Growth Des 2016;16:4318-26.
CROSSREF
2. Kim DH, Kim KI, Yoon S, Kim HJ, Ahn JS, Jun SH, et al. Dental hetero-graft materials with nano hydroxyapatite surface treatment. J Nanosci Nanotechnol 2015;15:7942-9.
PUBMED | CROSSREF
3. Richardson CR, Mellonig JT, Brunsvold MA, McDonnell HT, Cochran DL. Clinical evaluation of Bio-Oss®: a bovine-derived xenograft for the treatment of periodontal osseous defects in humans. J Clin Periodontol 1999;26:421-8.
PUBMED | CROSSREF
4. Tadic D, Epple M. A thorough physicochemical characterisation of 14 calcium phosphate-based bone substitution materials in comparison to natural bone. Biomaterials 2004;25:987-94.
PUBMED | CROSSREF
5. Hölzer A, Pietschmann MF, Rösl C, Hentschel M, Betz O, Matsuura M, et al. The interrelation of trabecular microstructural parameters of the greater tubercle measured for different species. J Orthop Res 2012;30:429-34.
PUBMED | CROSSREF
6. Lorenzen E, Follmann F, Jungersen G, Agerholm JS. A review of the human vs. porcine female genital tract and associated immune system in the perspective of using minipigs as a model of human genital Chlamydia infection. Vet Res 2015;46:116.
PUBMED | CROSSREF
7. Salamanca E, Lee WF, Lin CY, Huang HM, Lin CT, Feng SW, et al. A novel porcine graft for regeneration of bone defects. Materials (Basel) 2015;8:2523-36.
CROSSREF
8. Ramírez-Fernández M, Calvo-Guirado JL, Delgado-Ruiz RA, Maté-Sánchez del Val JE, Vicente-Ortega V, Meseguer-Olmos L. Bone response to hydroxyapatites with open porosity of animal origin (porcine [OsteoBiol®mp3] and bovine [Endobon®]): a radiological and histomorphometric study. Clin Oral Implants Res 2011;22:767-73.
PUBMED | CROSSREF
9. Go A, Kim SE, Shim KM, Lee SM, Choi SH, Son JS, et al. Osteogenic effect of low-temperature-heated porcine bone particles in a rat calvarial defect model. J Biomed Mater Res A 2014;102:3609-17.
PUBMED | CROSSREF

10. Mochalov KE, Efimov AE, Bobrovsky A, Agapov II, Chistyakov AA, Oleinikov V, et al. Combined scanning probe nanotomography and optical microspectroscopy: a correlative technique for 3D characterization of nanomaterials. ACS Nano 2013;7:8953-62.
PUBMED | CROSSREF
11. Mochalov KE, Efimov AE, Oleinikov VA, Nabiev I. High-resolution scanning near-field optical nanotomography: a technique for 3D multimodal nanoscale characterization of nano-biophotonic materials. Phys Procedia 2015;73:168-72.
CROSSREF
12. Mariotti F, Tomé D, Mirand PP. Converting nitrogen into protein--beyond 6.25 and Jones' factors. Crit Rev Food Sci Nutr 2008;48:177-84.
PUBMED | CROSSREF
13. Renders GA, Mulder L, van Ruijven LJ, van Eijden TM. Porosity of human mandibular condylar bone. J Anat 2007;210:239-48.
PUBMED | CROSSREF
14. Hing KA, Annaz B, Saeed S, Revell PA, Buckland T. Microporosity enhances bioactivity of synthetic bone graft substitutes. J Mater Sci Mater Med 2005;16:467-75.
PUBMED | CROSSREF
15. Lee DS, Pai Y, Chang S. Physicochemical characterization of InterOss® and Bio-Oss® anorganic bovine bone grafting material for oral surgery: a comparative study. Mater Chem Phys 2014;146:99-104.
CROSSREF
16. Lowell S, Shields JE. Powder surface area and porosity. 3rd ed. New York (NY): Springers; 1991.
17. Webb PA, Orr C. Analytical methods in fine particle technology. Norcross (GA): Micromeritics Instrument Corporation; 1997.
18. Lee H, Lee W, Lee JH, Yoon DS. Surface potential analysis of nanoscale biomaterials and devices using kelvin probe force microscopy. J Nanomater 2016;2016:4209130.
19. Figueiredo M, Henriques J, Martins G, Guerra F, Judas F, Figueiredo H. Physicochemical characterization of biomaterials commonly used in dentistry as bone substitutes--comparison with human bone. J Biomed Mater Res B Appl Biomater 2010;92:409-19.
PUBMED | CROSSREF
20. LeGeros RZ. Calcium phosphates in oral biology and medicine. Monogr Oral Sci 1991;15:1-201.
PUBMED | CROSSREF
21. Berzina-Cimdina L, Borodajenko N. Research of calcium phosphates using Fourier transform infrared spectroscopy. London: INTECH Open Access Publisher; 2012.
22. Rivera-Muñoz EM. Hydroxyapatite-based materials: synthesis and characterization. In: Fazel-Rezai R, editor. Biomedical engineering: frontiers and challenges. London: INTECH Open Access Publisher; 2011. Chapter 4.
23. Figueiredo MM, Gamelas JA, Martins AG. Characterization of bone and bone-based graft materials using FTIR spectroscopy. In: Theophanides T, editor. Infrared spectroscopy: life and biomedical sciences. London: INTECH Open Access Publisher; 2012. Chapter 18.
24. Sáez-Plaza P, Navas MJ, Wybraniec S, Michałowski T, Asuero AG. An overview of the Kjeldahl method of nitrogen determination. Part II. Sample preparation, working scale, instrumental finish, and quality control. Crit Rev Anal Chem 2013;43:224-72.
CROSSREF
25. Cohen SA, Strydom DJ. Amino acid analysis utilizing phenylisothiocyanate derivatives. Anal Biochem 1988;174:1-16.
PUBMED | CROSSREF
26. Crabb JW, West KA, Dodson WS, Hulmes JD. Amino acid analysis. Curr Protoc Protein Sci 2001;Chapter 11:Unit 11.9.
PUBMED
27. Cowin SC. Bone mechanics. Boca Raton (FL): CRC Press; 1989.
28. da Cruz AC, Pochapski MT, Daher JB, da Silva JC, Pilatti GL, Santos FA. Physico-chemical characterization and biocompatibility evaluation of hydroxyapatites. J Oral Sci 2006;48:219-26.
PUBMED | CROSSREF
29. Murugan R, Ramakrishna S, Panduranga Rao K. Nanoporous hydroxy-carbonate apatite scaffold made of natural bone. Mater Lett 2006;60:2844-7.
CROSSREF
30. Webster TJ, Ergun C, Doremus RH, Siegel RW, Bizios R. Enhanced functions of osteoblasts on nanophase ceramics. Biomaterials 2000;21:1803-10.
PUBMED | CROSSREF

31. Li X, van Blitterswijk CA, Feng Q, Cui F, Watari F. The effect of calcium phosphate microstructure on bone-related cells *in vitro*. Biomaterials 2008;29:3306-16.
PUBMED | CROSSREF

32. Kubies D, Himmlová L, Riedel T, Chánová E, Balík K, Douděrová M, et al. The interaction of osteoblasts with bone-implant materials: 1. The effect of physicochemical surface properties of implant materials. Physiol Res 2011;60:95-111.
PUBMED

33. Rupp F, Gittens RA, Scheideler L, Marmur A, Boyan BD, Schwartz Z, et al. A review on the wettability of dental implant surfaces I: theoretical and experimental aspects. Acta Biomater 2014;10:2894-906.
PUBMED | CROSSREF